DOI: 10.1002/chem.201000045

Supramolecular Tetrad of Subphthalocyanine–Triphenylamine–Zinc Porphyrin Coordinated to Fullerene as an “Antenna-Reaction-Center” Mimic: Formation of a Long-Lived Charge-Separated State in Nonpolar Solvent

Mohamed E. El-Khouly,[a] Dong Kyu Ju,[b] Kwang-Yol Kay,*[b] Francis D’Souza,*[c] and Shunichi Fukuzumi*[a, d]

Abstract: We report here the formation of a long-lived charge-separated state of a self-assembled donor–acceptor tetrad, formed by axial coordination of a fulleropyrrolidine appended with an imidazole coordinating ligand (C_{60}Im) to the zinc center of a subphthalocyanine–triphenylamine–zinc porphyrin (SubPc–TPA–ZnP), as a charge-stabilizing antenna reaction center mimic in toluene. The subphthalocyanine and triphenylamine entities, with their high-energy singlet states, act as an energy-transferring antenna unit to produce a singlet zinc porphyrin. The formation constant for the self-assembled tetrad was determined to be $1.0\times10^4\,\mathrm{M}^{-1}$, suggesting a moderately stable complex formation. The geometric and electronic structures of the covalently linked SubPc–TPA–ZnP triad and self-assembled SubPc–TPA–ZnP:C_{60}Im tetrad were examined by using an ab initio B3LYP/6-31G method. The majority of the highest occupied frontier molecular orbital was found over the ZnP and TPA entities, whereas the lowest unoccupied molecular orbital was located over the fullerene entity, suggesting the formation of the radical-ion pair (SubPc–TPA–ZnP$^{\bullet+}$:C_{60}Im$^{\bullet-}$). The redox measurements revealed that the energy level of the radical-ion pair in toluene is located lower than that of the singlet and triplet states of the zinc porphyrin and fullerene entities. The femtosecond transient absorption measurements revealed fast charge separation from the singlet porphyrin to the coordinated C_{60}Im with a lifetime of 1.1 ns. Interestingly, slow charge recombination ($1.6\times10^5\,\mathrm{s}^{-1}$) and the long lifetime of the charge-separated state (6.6 μs) were obtained in toluene by utilizing the nanosecond transient measurements.

Keywords: artificial photosynthesis · electron transfer · fullerenes · porphyrinoids · subphthalocyanines · supramolecular chemistry

Introduction

The X-ray structures of the bacterial photosynthetic reaction centers have revealed that the electron donor and acceptor entities are arranged through noncovalent incorporation into a well-defined protein matrix.[1] The light-induced electron transfer and energy transfer events occur between these well-organized pigments with a high quantum efficien-

---

[a] Dr. M. E. El-Khouly, Prof. Dr. S. Fukuzumi
Department of Material and Life Science
Graduate School of Engineering
Osaka University
SORST, Science and Technology Agency (JST)
Suita, Osaka 565-0871 (Japan)
Fax: (+81) 6-6879-7370
E-mail: fukuzumi@chem.eng.osaka-u.ac.jp

[b] D. K. Ju, Prof. Dr. K.-Y. Kay
Department of Molecular Science and Technology
Ajou University, Suwon 443-749 (South Korea)
Fax: (+82) 31-219-1615
E-mail: kykay@ajou.ac.kr

[c] Prof. Dr. F. D’Souza
Department of Chemistry
Wichita State University
1845 Fairmount, Wichita, KS, 67260-0051 (USA)
Fax: (+1) 316-978-3431
E-mail: Francis.dsouza@wichita.edu

[d] Prof. Dr. S. Fukuzumi
Department of Bioinspired Science
Ewha Womans University
Seoul 120-750 (South Korea)

Supporting information for this article is available on the WWW under http://dx.doi.org/10.1002/chem.201000045.

cy.[1] Owing to their importance in light-energy harvesting and developing optoelectronic devices, development of relatively simple donor–acceptor model systems designed to mimic the events of the photosynthetic reaction center has been one of the important goals of chemistry during the past two decades.[2–15] More recently, researchers have begun incorporating not only the 'reaction center' electron-transfer functionality, but also the energy transfer 'antenna' functionality into artificial photosynthetic constructs. In the developed artificial systems, energy-funneling antenna molecules have been elegantly connected to the donor–acceptor systems to probe sequential energy- and electron-transfer processes, thus mimicking the complex "antenna-reaction center" functionality of photosynthesis.

Although a substantial amount of progress in terms of charge stabilization has been accomplished in covalently linked donor–acceptor systems, achieving similar results on a self-assembled donor–acceptor has been challenging because of the occurrence of multiple equilibrium processes and the inferior stability of the adopted self-assembly approaches.[15] In the hope of finding a long-lived charge-separated state in the self-assembled systems, we report here a novel example of a triad and tetrad comprising porphyrin, triphenylamine, subphthalocyanine, and fullerene entities, as antenna-reaction center mimics (Figure 1). The rationale for choosing the different entities and the design concepts are as follows: porphyrin, the pigment of life, is a suitable primary electron donor owing to its resemblance to the natural photosynthetic chlorophyll pigment, easy synthetic manipulations, extensive absorption, and favorable redox properties.[16] To increase the donor ability of zinc porphyrin (lowering the oxidation potential), the electron-rich triphenylamine (TPA) entity is substituted at the *meso* position of the zinc–porphyrin ring. Owing to the close proximity of the TPA entity to the porphyrin π ring, delocalization of the porphyrin π system over the triphenylamine entity is expected.[17] The comparatively electron-deficient, subphthalocyanine, SubPc, in **1** plays the role of the antenna unit. The SubPc entity possesses i) strong absorption in the visible region ($\lambda = 500$–700 nm), ii) higher energy of the singlet excited state (2.16 eV) and triplet excited state (1.40 eV) compared with those of phthalocyanines, and iii) relatively low reorganization energies.[13,14] The covalently linked subphthalocyanine–triphenylamine–zinc porphyrin **1**, owing to the presence of three chromophores absorbing different portions of the visible spectrum, guarantees an increased absorption cross-section and an efficient use of the solar energy. Finally, fullerene,[18] the ultimate electron acceptor,[8–15] has been utilized to construct the supramolecular tetrad **2** by a self-assembly approach involving axial coordination.[15] Here, an imidazole-appended fullerene has been chosen over the pyridine-appended fullerene because of its increased ability to form stable coordination bonds with metal ions in the porphyrin cavity.[15,20] The presence of fullerene is expected to stabilize the charge-separated state, owing to favorable energy states and low-reorganization energy.[21]

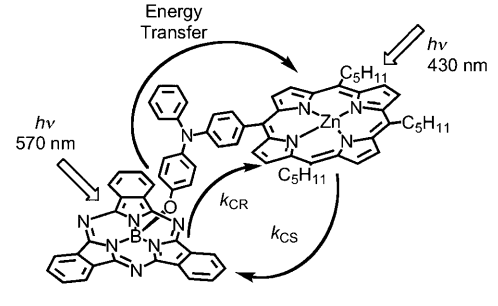

SubPc-TPA-ZnP, 1

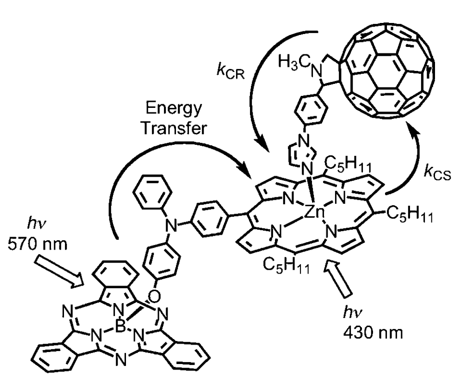

SubPc-TPA-ZnP:C_{60}Im, 2

Figure 1. Structures of the presently developed and investigated SubPc–TPA–ZnP triad **1** and the self-assembled SubPc–TPA–ZnP:C_{60}Im tetrad **2**.

The electron-transfer process from the electron-donating ZnP and TPA entities to the electron-accepting subphthalocyanine to form $SubPc^{\bullet-}$–TPA–$ZnP^{\bullet+}$ in **1** is confirmed in this study by different photochemical techniques. To achieve a long-lived charge-separate state in nonpolar toluene, the self-assembled tetrad **2** is formed in toluene (Figure 1). Owing to the varying redox and optical properties of the different entities of the tetrad, several interesting properties are envisioned in the tetrad: i) the subphthalocyanine entity with its higher singlet state (2.16 eV) is expected to act as an energy-transferring antenna unit to the zinc porphyrin and to promote electron transfer to the electron-accepting fullerene entity, ii) the triphenylamine entity with its higher singlet state (2.55 eV) is also expected to be an energy-transferring antenna unit to the zinc porphyrin in addition to stabilizing the charge-separated state,[17] and iii) owing to the lower energy level of the radical-ion pair SubPc–TPA–$ZnP^{\bullet+}$:$C_{60}Im^{\bullet-}$ compared to the lowest excited singlet and triplet states of both porphyrin and fullerene entities in nonpolar toluene, formation of a long-lived charge-separated state of SubPc–TPA–$ZnP^{\bullet+}$:$C_{60}Im^{\bullet-}$ is expected. The latter is not a common feature in the case of ZnP–C_{60} dyads, owing to the undesired charge recombination of the radical-ion pair to the low-lying triplet states of porphyrin and fullerene.[15,20,21] The photochemical processes were examined in nonpolar toluene, keeping in consideration that the protein environment surrounding the photosynthetic reaction center is nonpolar with a low dielectric constant $\varepsilon \approx 2.25$.

Results and Discussion

Synthesis and characterization: Subphthalocyanine–triphenylamine–zinc porphyrin (**1**) and its reference compounds, ZnP–TPA (**12**) and ZnP (**3**) were prepared, as depicted in Scheme 1. Every step of the reaction sequence proceeded smoothly to give a good or moderate yield of the product. Briefly, commercially available diphenylamine was coupled with 4-iodoanisole under Ullmann conditions[22] to give 4-methoxytriphenylamine (**4**) in 86 % yield, and subsequently Vilsmeier formylation[23] was carried out to produce aldehyde **5** in 94 % yield. Metal-free asymmetrical porphyrin **6** was prepared according to a typical method for porphyrin synthesis[24] in a yield of 8 %, and subsequent demethylation of the methoxy group in **6** was performed by using BBr_3 to give porphyrin **7** in 69 % yield. The hydroxy group in **7** replaced the axial chlorine atom of SubPc-Cl, which was synthesized according to the literature procedures,[13,14] to produce SubPc–TPA–H_2P **8** in 10 % yield. Finally, metalation was carried out using zinc acetate to afford SubPc–TPA–ZnP **1** in 82 % yield. Reference compounds ZnP-TPA **12** and ZnP **3** were also synthesized in a similar way, and SubPc-TPA was prepared according to the method previously reported by our group.[13]

Computational studies: To gain insight into the molecular geometry and electronic structure, computational studies were performed by using the ab initio B3LYP/6-31G method. In the optimized structure of **1** (see Figure S1 in the Supporting Information), the center-to-center distance (d_{CC}) between the Zn center and the B center of SubPc was 13.6 Å. The electron cloud of the highest occupied frontier molecular orbital (HOMO) was delocalized over the porphyrin macrocycle and the triphenylamine entities, while the lowest unoccupied molecular orbital (LUMO) was fully localized over the SubPc entity. These results suggest that the TPA–ZnP act as electron donors, whereas the SubPc acts as an electron acceptor, to afford $SubPc^{\bullet -}$–TPA–$ZnP^{\bullet +}$.

When C_{60}Im is axially coordinated with ZnP–TPA–SubPc (Figure 2), the center-to-center distances between the C_{60}Im

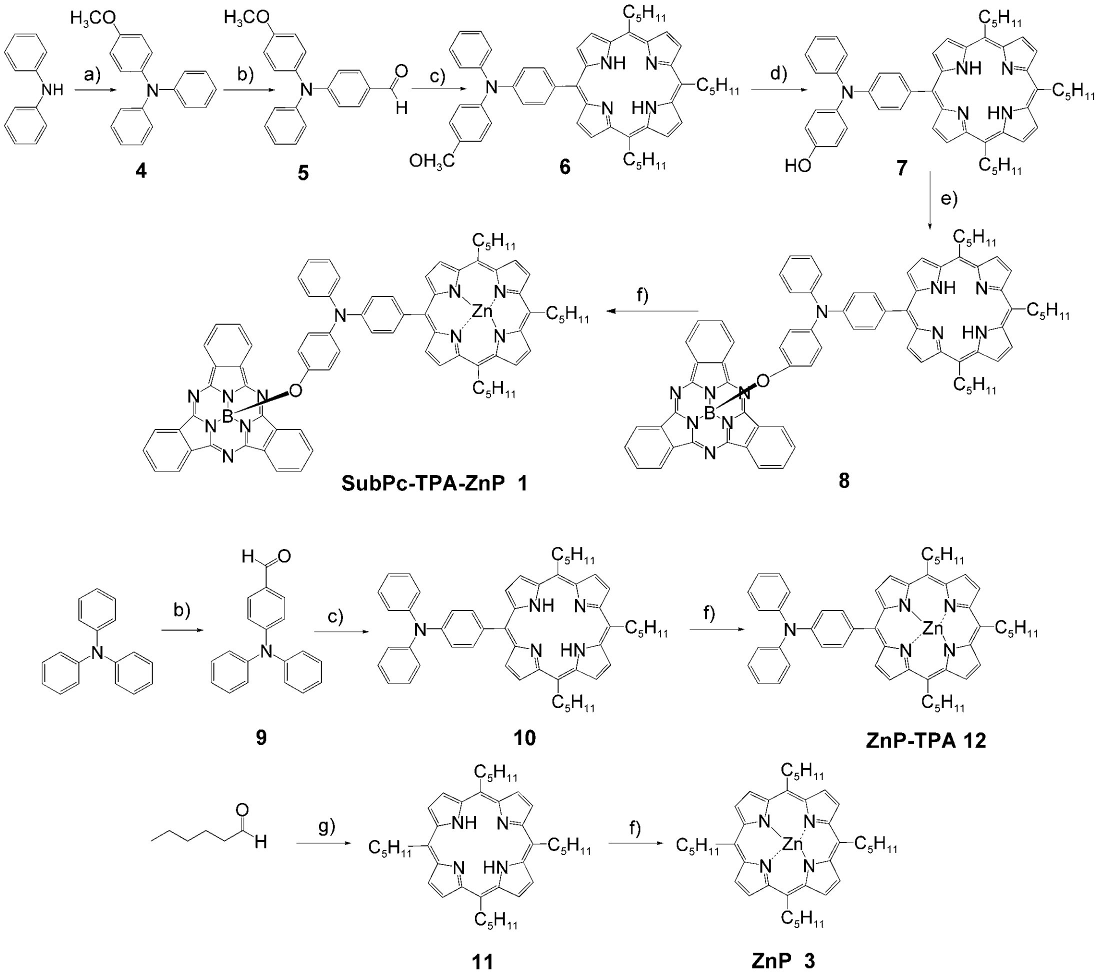

Scheme 1. Synthesis of compounds **1**, **2**, and **3**. a) K_2CO_3, Cu, [18]crown-6, *o*-dichlorobenzene, 180 °C, 36 h, 86 %; b) $POCl_3$, DMF, 1,2-dichloroethane, reflux, 4 h, 94 % for **5**, 12 h, 85 % for **9**; c) 1) hexanal, pyrrole, $BF_3{\cdot}O(C_2H_5)_2$, 2) DDQ, triethylamine, 2-propanol, dichloromethane, RT, 3 h, 8 % for **6** and **10**; d) BBr_3, dichloromethane, RT, 12 h, 69 %; e) SubPc-Cl, toluene, reflux, 6 days, 10 %; f) zinc acetate, dichloromethane, methanol, RT, 1 h, 82 % for **1**, 92 % for **12**, and 88 % for **3**; g) 1) pyrrole, $BF_3{\cdot}O(C_2H_5)_2$, 2) DDQ, 2-propanol, dichloromethane, RT, 3 h, 11 %.

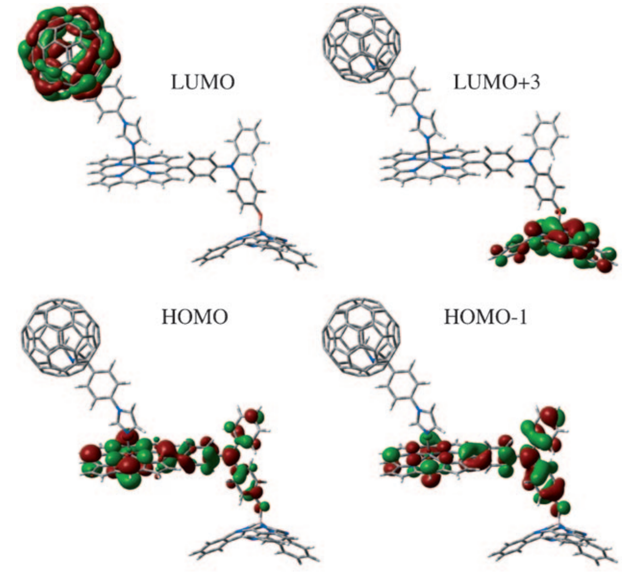

Figure 2. Frontier HOMO and LUMO orbitals of self-assembled **2**.

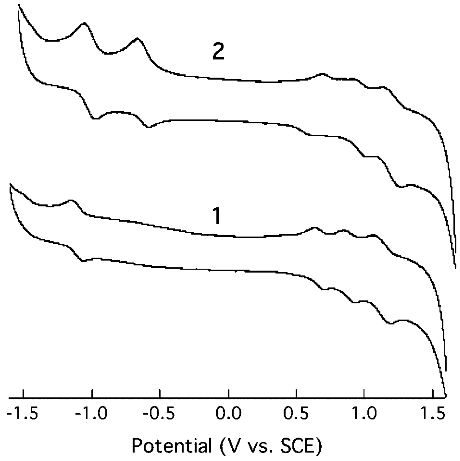

Figure 3. Cyclic voltammograms of **1** and self-assembled **2** in CH_2Cl_2 containing 0.1 M $(n\text{-}C_4H_9)_4NClO_4$. Scan rate = 100 mV s^{-1}.

and ZnP and SubPc of the formed supramolecular system were computed to be 11.7 and 22.7 Å, respectively. The electron cloud of the HOMO and HOMO−1 were delocalized over the porphyrin macrocycle and the substituted triphenylamine entities, whereas the LUMO and LUMO+3 were fully localized over the C_{60}Im and SubPc entities, respectively. These results suggest that the ZnP and TPA act as electron donors, whereas the C_{60}Im acts as an electron acceptor, to afford SubPc–TPA–ZnP$^{\bullet+}$:C_{60}Im$^{\bullet-}$ as the final charge-separated state. The orbital energies of the HOMO, HOMO−1, LUMO, and LUMO+3 were found to be −4.41, −4.70, −3.26, and −2.60 eV for the SubPc–TPA–ZnP:C_{60}Im. The calculated values of the HOMO–LUMO and HOMO–LUMO+3 gaps (gas phase) were found to be 1.16 and 1.81 eV, respectively, which are in a good agreement with the electrochemically measured (difference between the first oxidation and first reduction potential) values, as discussed below.

Electrochemical studies and electron transfer driving forces: The redox measurements were carried out by using cyclic voltammogram (CV) and differential pulse voltammogram (DPV) techniques in deaerated dichloromethane (CH_2Cl_2) to estimate the driving forces for the electron-transfer processes. The first oxidation potential (E_{ox}) of **12** is located at 690 mV versus SCE that is less positive by 20 mV compared to **3** (see Figures S2 and S3 in the Supporting Information), suggesting that the triphenylamine unit slightly improves the electron-donor ability of ZnP. The redox measurements of **1** show the first oxidation of the ZnP and the first reduction potential (E_{red}) of SubPc at 666 and −1111 mV versus SCE, respectively (Figure 3). Based on the first E_{ox} and E_{red} values, the driving forces for the charge recombination ($-\Delta G_{CR}$) of SubPc$^{\bullet-}$–TPA–ZnP$^{\bullet+}$ to the ground state were calculated as 1.57, 1.77, and 1.89 eV in benzonitrile, *o*-dichlorobenzene, and toluene, respectively.[25] Based on the $-\Delta G_{CR}$ value, the driving forces of the charge-separation process ($-\Delta G_{CS}{}^{S}$) through the singlet porphyrin (2.06 eV) were estimated to be 0.49, 0.29, and 0.17 eV in benzonitrile, *o*-dichlorobenzene, and toluene, respectively.[25]

On the other hand, the redox measurements of self-assembled **2** exhibited the first oxidation potential of ZnP and the first reduction of C_{60}Im and SubPc at 578, −689, and −1078 mV versus SCE, respectively (Figure 3 and Figure S4 in the Supporting Information). From these findings, the penta-coordinated ZnP formed by coordination of C_{60}Im with a Zn atom is found to be less positive than the ZnP of **1** by 88 mV (versus SCE), suggesting an increased electron-donor ability of ZnP when photoinduced charge separation takes place in **2**.[26] From these values, the $-\Delta G_{CR}$ and $-\Delta G_{CS}{}^{S}$ values of the stabilized charge-separated SubPc–TPA–ZnP$^{\bullet+}$:C_{60}Im$^{\bullet-}$ were estimated as 1.36 and 0.70 eV, respectively, in toluene. The finding that the energy level of SubPc–TPA–ZnP$^{\bullet+}$:C_{60}Im$^{\bullet-}$ is lower than the energy of both the triplet porphyrin (1.55 eV) and C_{60} (1.53 eV) suggests the exothermic electron transfer via the triplet porphyrin ($-\Delta G_{CS}{}^{T} = 0.17$ eV) and fullerene ($-\Delta G_{CS}{}^{T} = 0.15$ eV) in toluene.

Steady-state UV/Vis spectral studies: As shown in Figure 4, the absorption spectra of the reference SubPc consist of a high-energy B-band ($\lambda = 311$ nm) and lower energy Q-bands ($\lambda = 518$ and 565 nm) arising from π–π* transitions, which are associated with 14 π-electron systems, analogous to those of porphyrins and phthalocyanines. The absorption spectra of the **3** exhibited a Soret band at $\lambda = 423$ nm and Q-bands at $\lambda = 557$ and 599 nm, whereas the absorption band of TPA was located at $\lambda = 303$ nm. In agreement with the MO calculations and redox measurements, the ZnP Soret band of **12** was red shifted by nearly 4 nm compared with that of **3**, suggesting interactions between the porphyrin π system and the substituted triphenylamine entity. The electronic absorption spectra of **1** displayed common features of

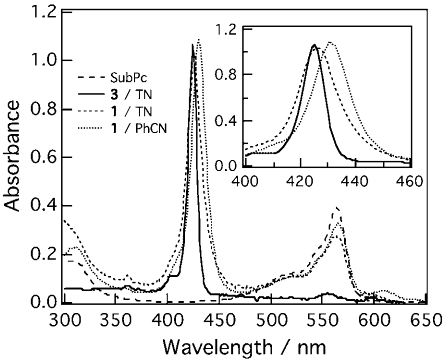

Figure 4. Steady-state absorption spectra of **1** and the reference compounds in toluene.

the electron-donor ZnP–TPA and the electron-acceptor SubPc subunits, suggesting the absence of electronic interactions between them in the ground state. Changing the solvent to benzonitrile shifted the absorption spectrum to red by about 5 nm compared to that in toluene and dichlorobenzene.

Upon coordination of C_{60}Im with **1**, the formation of the pentacoordinated zinc porphyrin complex was characterized by a diminished Soret band intensity, a 4 nm red-shift, and the appearance of an isosbestic point at $\lambda = 430$ nm. This observation suggests that the imidazole unit attached to the C_{60} was involved in coordination with the Zn atom, forming self-assembled **2** (Figure 5). No new absorption bands in the near IR region were observed, suggesting the absence of π–π type interactions between them. The Benesi–Hildebrand plot[27] constructed from the absorbance data revealed a straight line with $K = 1.1\times10^4\,\text{M}^{-1}$ (see Figure 5 inset), indicating stable complex formation. The binding constant of the self-assembled **2** is considerably high compared with many-studied axial ligands.[28]

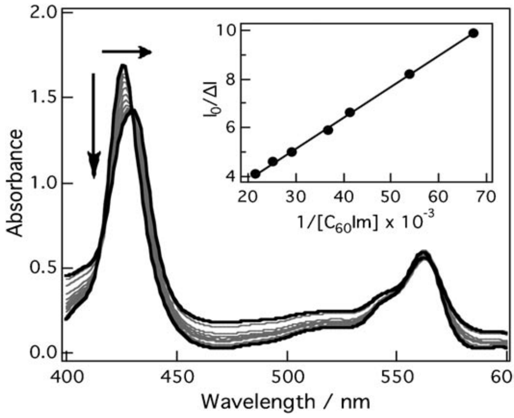

Figure 5. UV/Vis spectral changes observed during the complexation of **1** with C_{60}Im in toluene. Inset: Benesi–Hildebrand plot for the change of absorbance at $\lambda = 426$ nm constructed to obtain the binding constant.

Emission studies: The photophysical behavior was first investigated using steady-state fluorescence. When the most intense visible band at $\lambda = 430$ nm was excited, the fluorescence spectra of **12** revealed emission bands at $\lambda = 605$ and 653 nm. In the case of **1**, the emission intensity of the ZnP moiety was significantly quenched in benzonitrile, *o*-dichlorobenzene, and toluene (Figure 6). These observations together with the calculated negative ΔG_{CS} values from ^{1}ZnP*, suggest that the charge-separation process occurs from the electron-donating ^{1}ZnP* to the electron-accepting SubPc, generating SubPc$^{\bullet -}$–TPA–ZnP$^{\bullet +}$ in both polar and nonpolar solvents.

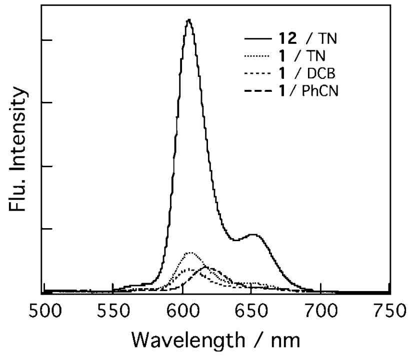

Figure 6. Fluorescence spectra of **12** in toluene and **1** in different solvents; $\lambda_{ex} = 430$ nm.

When the SubPc was selectively excited at $\lambda = 470$–580 nm, the emission band of ^{1}SubPc*–TPA–ZnP around $\lambda = 571$ nm was significantly quenched compared to that of the SubPc reference (see Figure S5 in the Supporting Information). With the decrease in the fluorescence intensity of SubPc, we could detect the emission bands of the ZnP entity, which were not clearly observed for the ZnP reference within this range of excitation wavelengths under the experimental conditions. This suggests that the observed porphyrin emission is a result of energy transfer from the singlet subphthalocyanine (2.16 eV) to the singlet porphyrin (2.06 eV). Excitation spectra of **1**, recorded by fixing the emission monochromator to the porphyrin emission maximum in the range of $\lambda = 580$–670 nm, revealed a subphthalocyanine absorption in addition to ZnP absorption bands (see Figure S6 in the Supporting Information). This observation confirms that the observed porphyrin emission is a result of singlet energy transfer from the subphthalocyanine entity to the porphyrin.

The fluorescence lifetime measurements support the considerations derived from the steady-state fluorescence spectra in a more quantitative way (see Figure S7 in the Supporting Information). The ZnP reference exhibited monoexponential decay with a lifetime (τ_f) of 2080 ps, which is in a good agreement with the reported value. In the case of **1**, the fluorescence decay-time profile of ZnP was fitted satisfactorily with mono-exponential decay with a lifetime of less than 100 ps. Such a shortening of the fluorescence lifetime indicates the occurrence of charge separation via the singlet ZnP to the attached SubPc, generating SubPc$^{\bullet -}$–TPA–ZnP$^{\bullet +}$. Based on the fluorescence lifetimes of the SubPc–TPA–^{1}ZnP* and ZnP reference, the rates of fluorescence quenching ($k_q{}^S$) were evaluated to be as much as 10^{10} s^{-1} in both polar benzonitrile and nonpolar toluene.

Upon addition of C$_{60}$Im to a solution of **1** in toluene, the fluorescence intensity of the singlet ZnP was significantly quenched (see Figure S8 in the Supporting Information). Scanning the emission wavelength to longer wavelength regions (λ = 700–775 nm) revealed no emission of the fulleropyrrolidine moiety at λ = 720 nm. The ZnP emission intensity decreased as the concentration of the fulleropyrrolidine increased, suggesting the occurrence of electron transfer from the singlet ZnP to C$_{60}$Im. The binding constant for the supramolecular complex formation was evaluated by constructing a Benesi–Hildebrand plot of the quenching data. As shown in the inset of Figure S8 in the Supporting Information, the calculated binding constant was found to be 1.1×10^4 M^{-1}, a value close to that calculated from the optical data shown in Figure 5, suggesting a moderately stable complex formation.

Femtosecond and nanosecond transient absorption measurements: Spectroscopic evidence for the occurrence of electron transfer in **1** was obtained from femtosecond transient absorption measurements in benzonitrile and toluene (Figure 7) by using 430-nm laser light, with which the ZnP moiety is selectively excited. In the time-resolved spectrum at 1 ps, the absorption band at λ = 470 nm is assigned to ^{1}ZnP*, whereas the spectra at >6 ps, which show absorption peaks in the visible region, are ascribed to the formation of the radical-ion pair SubPc$^{\bullet -}$–TPA–ZnP$^{\bullet +}$. The time-profile of TPA–ZnP$^{\bullet +}$ in the visible region (Figure 7, inset) shows a fast rise, from which the rate of the charge-separation process ($k_{CS}{}^S$) via ^{1}ZnP* was calculated to be 8.9×10^{10} s^{-1}. On the other hand, the decay-profile of TPA–ZnP$^{\bullet +}$ was observed, as shown in inset of Figure 8, from which the rate constant of the charge-recombination process (k_{CR}) and the lifetime of the radical-ion pair ($\tau_{RIP} = 1/k_{CR}$) were evaluated to be 3.9×10^9 s^{-1} and 256 ps, respectively. When changing the solvent to toluene, the k_{CR} and τ_{RIP} values were evaluated to be 7.1×10^9 s^{-1} and 140 ps, respectively. These results are qualitatively in agreement with a charge-recombination processes occurring in the normal region of the Marcus plot.[29–31]

The femtosecond transient absorption measurements of the self-assembled tetrad **2** in nonpolar toluene showed the absorption of TPA–ZnP$^{\bullet +}$ in the visible region between 650 and 800 nm, together with the near-IR absorption of C$_{60}$Im$^{\bullet -}$ with a maximum at λ = 1000 nm, confirming the formation of the radical ion pair SubPc–TPA–ZnP$^{\bullet +}$:C$_{60}{}^{\bullet -}$. The time-profile of C$_{60}$Im$^{\bullet -}$ in the NIR region (Figure 7, inset) shows a fast rise, from which the rate of the charge-separation process ($k_{CS}{}^S$) from the singlet ZnP to C$_{60}$Im was calculated as 8.0×10^{11} s^{-1}. The k_{CR} and τ_{RIP} values were evaluated to be 6.3×10^8 s^{-1} and 1.1 ns, respectively.

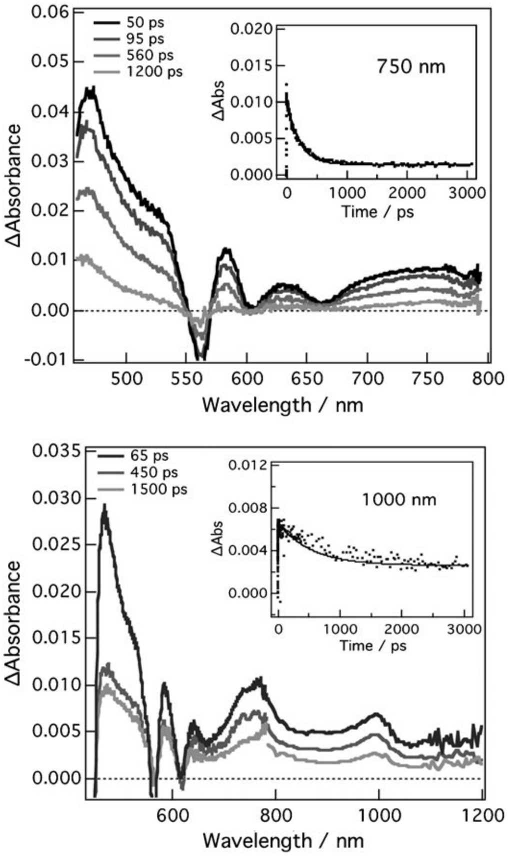

Figure 7. Differential transient absorption spectra obtained upon femtosecond photoexcitation (λ = 430 nm) of **1** (upper) and self-assembled **2** (lower) in deaerated toluene. λ_{ex} = 430 nm.

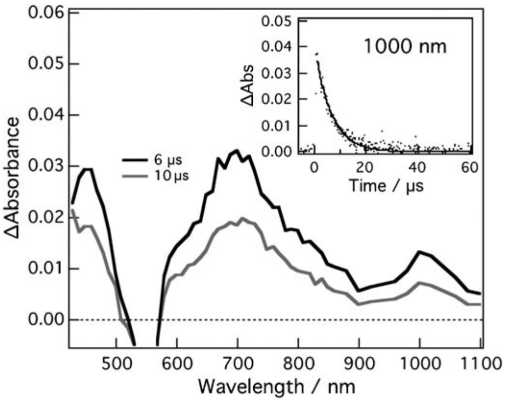

Figure 8. Nanosecond transient spectra of self-assembled **2** in deaerated toluene. λ_{ex} = 430 nm.

Nanosecond transient absorption measurements: The nanosecond transient spectra of the reference **12** in toluene, by employing 430-nm laser light, exhibited the absorption of triplet ZnP at λ = 450 nm. The triplet-state decayed to the ground state with a rate of 1.0×10^4 s^{-1}. In the case of **1**, the recorded absorption spectra in both benzonitrile and toluene are similar to that of ZnP, suggesting the absence of electron transfer via triplet ZnP (see Figure S9 in the Supporting Information). The absorption intensity of SubPc–TPA–^{3}ZnP* was significantly decreased compared with the triplet ^{3}ZnP* and decayed with a rate of 1.0×10^4 s^{-1}.

In the case of self-assembled **2**, it was interesting to detect the transient absorption bands of TPA–ZnP$^{\bullet+}$ in the visible region (see Figure S10 in the Supporting Information) and C_{60}Im$^{\bullet-}$ in the NIR region in the microseconds region (Figure 8). This observation demonstrates the generation of the radical-ion pair in toluene. From the energetic point of view, the electron transfer from the triplet porphyrin to the attached C_{60}Im in toluene is exothermic. The decay of C_{60}Im$^{\bullet-}$ was fit by first-order kinetics, suggesting the absence of the bimolecular electron-transfer process. The k_{CR} and τ_{RIP} values of SubPc–TPA–ZnP$^{\bullet+}$:C_{60}Im$^{\bullet-}$ were estimated to be 1.6×10^6 s^{-1} and 6.6 μs, respectively. We believe that this long-lived charge-separated state is a consequence of the persistence of the triplet-correlated radical-ion pair character, which results in the corresponding forbidden character of the charge recombination back to the singlet ground state. In other words, the triplet multiplicity of the radical ion-pair, which is populated from the electron transfer from the triplet porphyrin to the attached C_{60}Im, plays an important role in determining its long lifetime. The quick decay of the radical species in oxygen-saturated toluene confirms the triplet-spin character of the SubPc–TPA–ZnP$^{\bullet+}$:C_{60}Im$^{\bullet-}$.

The energy-level diagrams, shown in Figure 9, summarize the observed intramolecular events of **1** and the self-assembled **2**. The energy level of the radical-ion pair, SubPc–TPA–ZnP$^{\bullet+}$:C_{60}Im$^{\bullet-}$, which was calculated by using E_{ox}, E_{red}, and the center-to-center distance (R_{CC}), is found to be lower than the level of the excited singlet and triplet states of both ZnP and C_{60}Im. The electron transfer via the singlet ZnP was observed by the femtosecond laser spectral measurements in the order of picoseconds. Interestingly, the unusual long-lived charge-separated state of SubPc–TPA–ZnP$^{\bullet+}$:$C_{60}^{\bullet-}$ in the order of microseconds was clearly observed in toluene. From a point of view of mechanistic information, the advantage of supramolecular **1**:C_{60}Im is that both the lifetimes of the singlet and triplet SubPc–TPA–ZnP$^{\bullet+}$:C_{60}Im$^{\bullet-}$ could be determined.

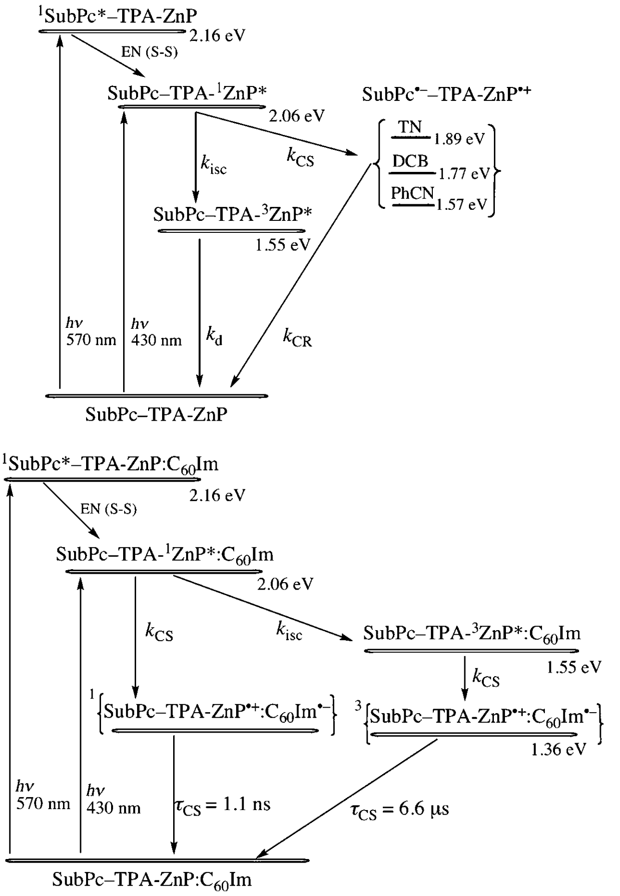

Figure 9. Energy level diagrams of **1** in different solvents and self-assembled **2** in toluene. $\lambda_{ex}=430$ nm.

Conclusion

The synthesis, characterization, and photochemical events in the molecular triad, SubPc–TPA–ZnP, comprising a subphthalocyanine, triphenylamine, and a zinc porphyrin, is described. Excitation of SubPc in the triad resulted in efficient energy transfer to the ZnP entity. By utilizing femtosecond laser photolysis, the electron transfer from the singlet ZnP, which is generated either by energy transfer from SubPc or through direct excitation, to the electron-accepting SubPc was observed, forming SubPc$^{\bullet-}$–TPA–ZnP$^{\bullet+}$ with lifetimes of 256 and 140 ps in benzonitrile and toluene, respectively. The finding that the lifetime of SubPc$^{\bullet-}$–TPA–ZnP$^{\bullet+}$ is longer in polar benzonitrile than in nonpolar toluene suggests that the charge recombination is occurring in the normal region of the Marcus plot.

Interestingly, in the supramolecular tetrad **2**, obtained by axial coordination of C_{60}Im to ZnP–TPA–SubPc, we achieved the anticipated charge stabilization in nonpolar solvents. The formation constant for the self-assembled tetrad was determined to be 1.0×10^4 M^{-1}, suggesting a moderately stable complex formation. The electrochemical measurements revealed that the energy level of the radical-ion pair (SubPc–TPA–ZnP$^{\bullet+}$:C_{60}Im$^{\bullet-}$) is located lower than that of the singlet and triplet states of the zinc porphyrin and the fullerene entities. The geometric and electronic structures of the tetrad, examined by ab initio B3LYP/6-31G methods, revealed the HOMO to be over the ZnP and TPA entities, whereas the LUMO to be over the fullerene entity, suggesting that the formation of SubPc–TPA–ZnP$^{\bullet+}$-C_{60}Im$^{\bullet-}$ as the charge-separation products. The main quenching pathway involved electron transfer from the singlet excited ZnP to the C_{60}Im moiety. The rate constant of the forward electron transfer, k_{CS}, was determined to be 8×10^{11} s^{-1}. Interestingly, a slow charge recombination (1.6×10^5 s^{-1}) and the long lifetime of the charge-separated state (6.6 μs) were obtained in toluene by utilizing nanosecond transient measurements. The formation of a long-lived charge-separated state in the tetrad was interpreted as a consequence of the persistence of the triplet-correlated radical-ion pair character that is forbidden for charge recombination back to the singlet ground state.

Experimental Section

Materials and instruments: Reagents and solvents were purchased as reagent grade and used without further purification. All reactions were performed by using dry glassware under a nitrogen atmosphere. Analytical TLC was carried out on Merck 60 F254 silica gel plates, and column chromatography was performed on Merck 60 silica gel (230–400 mesh). Melting points were determined by using an Electrothermal IA 9000 series melting point apparatus and are uncorrected. NMR spectra were recorded by using a Varian Mercury-400 (400 MHz) spectrometer with a TMS peak as reference. UV/Vis spectra were recorded by using a Jasco V-550 spectrometer. MALDI-TOF MS spectra were recorded by using an Applied Biosystems Voyager-DE-STR. Elemental analyses were performed with a Perkin–Elmer 2400 analyzer. Steady-state fluorescence spectra were measured by using a Shimadzu RF-5300 PC spectrofluorophotometer equipped with a photomultiplier tube having high sensitivity in the $\lambda = 700$–800 nm region. Cyclic voltammograms were carried by using a BAS CV-50W Voltammetric Analyzer. A platinum disk electrode was used as working electrode, whereas a platinum wire served as a counter electrode. SCE electrode was used as a reference electrode. All measurements were carried out in CH_2Cl_2 containing 0.1 M (n-$C_4H_9)_4NClO_4$ as the supporting electrolyte. The scan rate = $100\ \mathrm{mV\,s^{-1}}$.

Laser flash photolysis: The studied compounds were excited by using a Panther OPO pumped by Nd:YAG laser (Continuum, SLII-10, 4–6 ns fwhm) at $\lambda = 430$ nm with the powers of 1.5 and 3.0 mJ per pulse. The transient absorption measurements were performed using a continuous xenon lamp (150 W) and an InGaAs-PIN photodiode (Hamamatsu 2949) as a probe light and a detector, respectively. The output from the photodiodes and a photomultiplier tube was recorded with a digitizing oscilloscope (Tektronix, TDS3032, 300 MHz). Femtosecond transient absorption spectroscopy experiments were conducted using an ultrafast source: Integra-C (Quantronix Corp.), an optical parametric amplifier: TOPAS (Light Conversion Ltd.) and a commercially available optical detection system: Helios provided by Ultrafast Systems LLC. The source for the pump and probe pulses were derived from the fundamental output of Integra-C (780 nm, 2 mJ/pulse and fwhm = 130 fs) at a repetition rate of 1 kHz. 75 % of the fundamental output of the laser was introduced into TOPAS which has optical frequency mixers resulting in tunable range from $\lambda = 285$ to 1660 nm, whereas the rest of the output was used for white light generation. Typically, 2500 excitation pulses were averaged for 5 s to obtain the transient spectrum at a set delay time. Kinetic traces at appropriate wavelengths were assembled from the time-resolved spectral data. All measurements were conducted at 298 K. The transient spectra were recorded by using fresh solutions in each laser excitation.

4-(Diphenylamino)anisole (4): Copper powder (1.50 g, 23.6 mmol), K_2CO_3 (6.55 g, 54.4 mmol), [18]crown-6 (0.31 g, 1.17 mmol), and diphenylamine (2.00 g, 11.8 mmol) were added to a solution of 4-iodoanisole (4.15 g, 17.7 mmol) in *o*-dichlorobenzene (20 mL). After refluxing the reaction mixture for 48 h, it was cooled to room temperature and filtered off. The filtrate was evaporated and the residue was washed with ethanol and recrystallized from ethanol to give compound **4** (1.43 g, 86 %) as a brown solid. M.p. 108–109 °C; ^{1}H NMR (400 MHz, $CDCl_3$): $\delta = 7.18$ (m, 4H), 7.05 (d, $J = 4.4$ Hz, 2H), 7.01 (d, $J = 4.8$ Hz, 4H), 6.92 (m, 2H), 6.82 (d, $J = 4.4$ Hz, 2H), 3.78 ppm (s, 3H); elemental analysis (%) calcd for $C_{19}H_{17}NO$: C 82.88, H 6.22, N 2.84; found: C 82.87, H 6.25, N 2.93.

4-{*N*-(4-Methoxyphenyl)-*N*-phenylamino}benzaldehyde (5): Compound **4** (2.0 g, 7.26 mmol), and carefully poured $POCl_3$ (2.77 mL, 30.28 mmol) were added to a solution of DMF (2.35 mL, 30.28 mmol) in 1,2-dichloroethane (20 mL). The mixture was refluxed for 4 h, cooled to room temperature, and poured into saturated aqueous sodium acetate solution (50 mL). The product was extracted with dichloromethane (3 × 50 mL), and the extract was dried over $MgSO_4$, and evaporated. The residue was chromatographed on silica gel with dichloromethane/*n*-hexane (3:1) to give compound **5** (2.15 g, 94 %) in a yellow solid. M.p. 86–87 °C; ^{1}H NMR (400 MHz, $CDCl_3$): $\delta = 9.74$ (s, 1H), 7.64 (d, $J = 4.8$ Hz, 2H), 7.31 (m, 2H), 7.14 (d, $J = 4.8$ Hz, 2H), 7.10 (m, 3H), 6.93 (d, $J = 4.8$ Hz, 2H), 6.88 (d, $J = 4.4$ Hz, 2H), 3.80 ppm (s, 3H); elemental analysis (%) calcd for $C_{20}H_{17}NO_2$: C 79.19, H 5.65, N 4.62; found: C 79.02, H 5.84, N 4.34.

5-[4-{*N*-(4-Methoxyphenyl)-*N*-phenylamino}phenyl]-10,15,20-tris(pentyl)-21H,23H-porphine (6): Boron trifluoride diethyl etherate (1.34 mL, 10.56 mmol) was added to a solution of compound **5** (2 g, 6.6 mmol), hexanal (2.4 mL, 19.8 mmol), and pyrrole (1.8 mL, 26.4 mmol) in a mixture of dichloromethane (2.6 L) and 2-propanol (17 mL). The mixture was stirred at room temperature for 90 min. 2,3-Dichloro-5,6-dicyano-1,4-benzoquinone (DDQ, 6 g, 26.4 mmol) was added and the mixture was stirred at room temperature for 70 min. Finally triethylamine (3.7 mL, 26.4 mmol) was added and the mixture was stirred for 30 min. The solvent was removed under reduced pressure and the product was chromatographed on silica gel with chloroform/*n*-hexane (3:2) to give compound **6** (0.42 g, 8 %) as a purple solid. M.p. 86 °C; ^{1}H NMR (400 MHz, $CDCl_3$): $\delta = 9.48$ (m, 4H), 9.37 (d, $J = 4.4$ Hz, 2H), 8.92 (d, $J = 4.8$ Hz, 2H), 7.96 (d, $J = 4.4$ Hz, 2H), 7.36 (m, 8H), 7.05 (m, 1H), 6.98 (d, $J = 8.8$ Hz, 2H), 4.94 (m, 6H), 3.87 (s, 3H), 2.53 (m, 6H), 1.77 (m, 6H), 1.55 (m, 6H), 0.98 (m, 9H), −2.64 ppm (s, 2H); elemental analysis (%) calcd for $C_{54}H_{59}N_5O$: C 81.68, H 7.49, N 8.82; found: C 81.43, H 7.64, N 8.64.

5-[4-{*N*-(4-Hydroxyphenyl)-*N*-phenylamino}phenyl]-10,15,20-tris(pentyl)-21H,23H-porphine (7): Boron tribromide (1.0 M solution in dichloromethane) (0.56 mL, 0.56 mmol) was added to a solution of compound **6** (200 mg, 0.38 mmol) in dichloromethane (7 mL) at 0 °C and stirred for 30 min. The reaction mixture was stirred at room temperature for 12 h, poured into water, and then extracted with dichloromethane (3 × 50 mL). The extract was dried over Na_2SO_4, and evaporated. The residue was chromatographed on silica gel with dichloromethane/methanol (100:1) to give compound **7** (204 mg, 69 %) as a purple solid. M.p. 107 °C; ^{1}H NMR (400 MHz, $CDCl_3$): $\delta = 9.48$ (m, 4H), 9.37 (d, $J = 4.8$ Hz, 2H), 8.92 (d, $J = 4.8$ Hz, 2H), 7.96 (d, $J = 4.0$ Hz, 2H), 7.35 (m, 8H), 7.06 (m, 1H), 6.91 (d, $J = 8.4$ Hz, 2H), 4.94 (m, 6H), 4.65 (s, 1H), 2.53 (m, 6H), 1.77 (m, 6H), 1.54 (m, 6H), 0.98 (m, 9H), −2.64 ppm (s, 2H); elemental analysis (%) calcd for $C_{53}H_{57}N_5O$: C 81.61, H 7.37, N 8.98; found: C 81.41, H 7.60, N 8.75.

SubPc-TPA-H_2P (8): Compound **7** (100 mg, 0.128 mmol) was added to a solution of SubPc-Cl (110 mg, 0.256 mmol) in toluene (4 mL), and the reaction solution was refluxed for six days. The reaction mixture was cooled to room temperature and the solvent was evaporated. The product was chromatographed on silica gel with dichloromethane to give compound **8** (15 mg, 10 %) as a purple solid. M.p. 122 °C; ^{1}H NMR (400 MHz, $CDCl_3$): $\delta = 9.52$ (m, 4H), 9.46 (d, $J = 4.8$ Hz, 2H), 8.97 (d, $J = 4.8$ Hz, 2H), 8.85 (m, 6H), 7.88 (m, 8H), 7.25 (m, 2H), 7.16 (m, 4H), 6.98 (m, 1H), 6.83 (d, $J = 8.4$ Hz, 2H), 5.46 (d, $J = 4.0$ Hz, 2H), 4.94 (m, 6H), 2.53 (m, 6H), 1.77 (m, 6H), 1.54 (m, 6H), 0.98 (m, 9H), −2.65 ppm (s, 2H); elemental analysis (%) calcd for $C_{77}H_{68}N_{11}BO$: C 78.76, H 5.84, N 13.12; found: C 78.61, H 6.11, N 12.98.

SubPc-TPA-ZnP (1): After blocking light, compound **8** (15 mg, 0.012 mmol) was added to a solution of zinc acetate (23 mg, 0.12 mmol) in dichloromethane/methanol (10:1, 5 mL), and stirred for 30 min. The solvent was removed under reduced pressure and then the product was chromatographed on silica gel with dichloromethane to give compound **1** (13 mg, 82 %) as a red solid. M.p. 146 °C; ^{1}H NMR (400 MHz, $CDCl_3$): $\delta = 9.53$ (m, 4H), 9.47 (d, $J = 4.8$ Hz, 2H), 8.98 (d, $J = 4.8$ Hz, 2H), 8.86 (m, 6H), 7.89 (m, 8H), 7.20 (m, 6H), 6.99 (m, 1H), 6.83 (d, $J = 8.8$ Hz, 2H), 5.45 (d, $J = 8.8$ Hz, 2H), 4.95 (m, 6H), 2.55 (m, 6H), 1.82 (m, 6H), 1.56 (m, 6H), 1.02 ppm (m, 9H); ^{13}C NMR ($CDCl_3$): δ = 151.45, 149.77, 149.70, 149.46, 149.21, 148.97, 148.11, 147.25, 141.43, 136.28, 135.16, 132.14, 131.15, 130.01, 129.33, 128.92, 128.77, 128.63, 126.82, 123.79, 122.39, 120.39, 120.05, 120.00, 119.33, 38.96, 35.96, 33.28, 30.11, 23.23, 14.67, 1.63, 0.48 ppm; UV/Vis (toluene): $\lambda_{max} = 308$, 432, 523, 562 nm; MS (MALDI-TOF); m/z: $C_{77}H_{66}BN_{11}OZn$ calcd: 1235.48; found 1235.75; elemental analysis (%) calcd for $C_{77}H_{66}BN_{11}OZn$: C 74.73, H 5.38, N 12.48; found: C 74.61, H 5.51, N 12.38.

4-(Diphenylamino)benzaldehyde (9): Triphenylamine (1.8 g, 7.57 mmol) and carefully poured $POCl_3$ (2.77 mL, 30.28 mmol) was added to a solution of DMF (2.35 mL, 30.28 mmol) in 1,2-dichloroethane (20 mL). The mixture was refluxed for 12 h, cooled to room temperature, and then poured into saturated aqueous sodium acetate solution (300 mL). The product was extracted with dichloromethane (3×50 mL) and the extract was dried over $MgSO_4$, and evaporated. The residue was chromatographed on silica gel with dichloromethane to give compound **9** (1.85 g, 85%) as a yellow solid. M.p. 132°C; ^1H NMR (400 MHz, $CDCl_3$): $\delta = 9.78$ (s, 1H), 7.64 (d, $J = 4.8$ Hz, 2H), 7.31 (t, $J = 7.6$ Hz, 4H), 7.14 (m, 6H), 6.98 ppm (d, $J = 8.0$ Hz, 2H); elemental analysis (%) calcd for $C_{19}H_{15}NO$: C 83.49, H 5.53, N 5.12; found: C 83.22, H 5.71, N 5.01.

5-{4-(*N*,*N*-Diphenylamino)phenyl}-10,15,20-tris(pentyl)-21H,23H-porphine (10): Boron trifluoride diethyl etherate (0.85 mL, 6.7 mmol) was added to a solution of compound **9** (1.14 g, 4.17 mmol), hexanal (1.54 mL, 12.5 mmol), and pyrrole (1.16 mL, 16.67 mmol) in a mixture of dichloromethane (1.65 L) and 2-propanol (17 mL). The mixture was stirred at room temperature for 90 min. DDQ (3.78 g, 16.6 mmol) was added and the mixture was stirred at room temperature for 70 min. Finally, triethylamine (3.7 mL, 26.4 mmol) was added and the mixture was stirred for 30 min. The product was chromatographed on silica gel with chloroform/*n*-hexane (3:2) to give compound **10** (253 mg, 8%) as a purple solid. M.p. 92°C; ^1H NMR (400 MHz, $CDCl_3$): $\delta = 9.47$ (m, 4H), 9.38 (d, $J = 4.8$ Hz, 2H), 8.92 (d, $J = 4.8$ Hz, 2H), 7.99 (d, $J = 4.0$ Hz, 2H), 7.40 (m, 10H), 7.12 (m, 2H), 4.95 (m, 6H), 2.53 (m, 6H), 1.78 (m, 6H), 1.55 (m, 6H), 0.98 (m, 9H), −2.65 ppm (s, 2H); elemental analysis (%) calcd for $C_{53}H_{57}N_5$: C 83.31, H 7.52, N 9.17; found: C 83.09, H 7.76, N 9.01.

[5-{4-(*N*,*N*-Diphenylamino)phenyl}-10,15,20-tris(pentyl)-21H,23H-porphinato]zinc, ZnP-TPA (12): After blocking light, compound **10** (210 mg, 0.28 mmol) was added to a solution of zinc acetate (504 mg, 2.75 mmol) in dichloromethane/methanol (10:1, 20 mL), and stirred for 1 h. The solvent was evaporated and then the product was chromatographed on silica gel with dichloromethane to give compound **2** (210 mg, 92%) as a purple solid. M.p. 112°C; ^1H NMR (400 MHz, $CDCl_3$): $\delta = 9.54$ (m, 4H), 9.48 (d, $J = 4.8$ Hz, 2H), 9.02 (d, $J = 4.8$ Hz, 2H), 8.01 (d, $J = 7.6$ Hz, 2H), 7.41 (m, 10H), 7.13 (m, 2H), 4.94 (m, 6H), 2.55 (m, 6H), 1.82 (m, 6H), 1.56 (m, 6H), 1.01 ppm (m, 9H); UV/Vis (toluene): $\lambda_{max} = 305$, 471, 558, 598 nm; elemental analysis (%) calcd for $C_{53}H_{55}N_5Zn$: C 76.93, H 6.70, N 8.46; found: C 76.81, H 6.91, N 8.28.

5,10,15,20-Tetrakis(pentyl)-21H,23H-porphine (11): Boron trifluoride diethyl etherate (0.85 mL, 6.7 mmol) was added to a solution of hexanal (2.05 mL, 16.67 mmol) and pyrrole (1.16 mL, 16.67 mmol) in a mixture of dichloromethane (1.65 L) and 2-propanol (17 mL). The mixture was stirred at room temperature for 90 min. DDQ (3.78 g, 16.6 mmol) was added and the mixture was stirred at room temperature for 70 min. Finally, triethylamine (2.35 mL, 16.7 mmol) was added and the mixture was stirred for 30 min. The solvent was evaporated and then the product was chromatographed on silica gel with chloroform/*n*-hexane (3:2) to give compound **11** (350 mg, 11%) as a purple solid. M.p. 112°C; ^1H NMR (400 MHz, $CDCl_3$): $\delta = 9.42$ (s, 8H), 4.92 (m, 8H), 2.50 (m, 8H), 1.78 (m, 8H), 1.55 (m, 8H), 0.99 (m, 12H), −2.63 ppm (s, 2H); elemental analysis (%) calcd for $C_{40}H_{54}N_4$: C 81.31, H 9.21, N 9.48; found: C 81.03, H 9.33, N 9.08.

[5,10,15,20-Tetrakis(pentyl)-21H,23H-porphinato]zinc; ZnP (3): After blocking light, compound **11** (200 mg, 0.33 mmol) was added to a solution of zinc acetate (605 mg, 3.3 mmol) in dichloromethane/methanol (10:1, 20 mL), and stirred for 1 h. The solvent was removed under reduced pressure and then the product was chromatographed on silica gel with dichloromethane to give compound **3** (189 mg, 88%) as a purple solid. M.p. 103°C; ^1H NMR (400 MHz, $CDCl_3$): $\delta = 9.12$ (s, 8H), 4.56 (m, 8H), 2.40 (m, 8H), 1.77 (m, 8H), 1.54 (m, 8H), 1.01 ppm (m, 12H). UV/Vis (toluene): $\lambda_{max} = 310$, 471, 559, 598 nm; elemental analysis (%) calcd for $C_{40}H_{52}N_4Zn$: C 73.43, H 8.01, N 8.56; found: C 73.21, H 8.13, N 8.33.

Acknowledgements

This work was supported by a Grant-in-Aid (No. 20108010) and the Global COE (center of excellence) program "Global Education and Research Center for Bio-Environmental Chemistry" of Osaka University from Ministry of Education, Culture, Sports, Science and Technology, Japan, KOSEF/MEST through WCU project (R31-2008-000-10010-0), the National Science Foundation (Grant Nos. 0804015 and EPS-0903806) and matching support from the State of Kansas through Kansas Technology Enterprise Corporation. K.-Y. Kay also acknowledges the financial support from Brain Korea 21 Program in 2008.

---

[1] a) *The Photosynthetic Reaction Center* (Eds.: J. Deisenhofer, J. R. Norris), Academic Press, San Diego, **1993**; b) J. Deisenhofer, O. Epp, K. Miki, R. Huber, H. Michel, *J. Mol. Biol.* **1984**, *180*, 385; c) R. A. Wheeler, *Introduction to the Molecular Bioenergetics of Electron, Proton, and Energy Transfer*, ACS, Washington, **2004**, pp. 1–6; d) "Electron Transfer in Photosynthesis": W. Leibl, P. Mathis in *Molecular to Global Photosynthesis* (Eds.: M. D. Archer, J. Barber), Imperial College Press, London, **2004**, p. 117.

[2] a) G. McLendon, R. Hake, *Chem. Rev.* **1992**, *92*, 481; b) F. D. Lewis, R. L. Letsinger, M. R. Wasielewski, *Acc. Chem. Res.* **2001**, *34*, 159; c) J. S. Connolly, J. R. Bolton, *Photoinduced Electron Transfer, Part D* (Eds.: M. A. Fox, M. Chanon), Elsevier, Amsterdam, **1988**, pp. 303–393.

[3] a) J. R. Miller, L. T. Calcaterra, G. L. Closs, *J. Am. Chem. Soc.* **1984**, *106*, 3047; b) G. L. Closs, J. R. Miller, *Science* **1988**, *240*, 440.

[4] a) M. R. Wasielewski, *Acc. Chem. Res.* **2009**, *42*, 1910; b) D. Gust, T. A. Moore, A. L. Moore, *Acc. Chem. Res.* **2009**, *42*, 1890; c) H. A. Kurreck, A. L. Moore, *Acc. Chem. Res.* **2001**, *34*, 40.

[5] a) M.-J. Blanco, M. C. Jimenez, J.-C. Chambron, V. Heitz, M. Linke, J.-P. Sauvage, *Chem. Soc. Rev.* **1999**, *28*, 293; b) V. Balzani, A. Juris, M. Venturi, S. Campagna, S. Serroni, *Chem. Rev.* **1996**, *96*, 759; c) V. Balzani, A. Credi, M. Venturi, *ChemSusChem* **2008**, *1*, 26.

[6] a) M. N. Paddon-Row, *Acc. Chem. Res.* **1994**, *27*, 18; b) J. W. Verhoeven, *Adv. Chem. Phys.* **1999**, *106*, 603; c) K. Maruyama, A. Osuka, N. Mataga, *Pure Appl. Chem.* **1994**, *66*, 867; d) A. Osuka, N. Mataga, T. Okada, *Pure Appl. Chem.* **1997**, *69*, 797; e) L. Sun, L. Hammarström, B. Åkermark, S. Styring, *Chem. Soc. Rev.* **2001**, *30*, 36.

[7] a) J. S. Sessler, B. Wang, S. L. Springs, C. T. Brown in *Comprehensive Supramolecular Chemistry* (Eds.: J. L. Atwood, J. E. D. Davies, D. D. MacNicol, F. Vogtle), Pergamon, New York, **1996**, Chapter 9; b) T. Hayashi, H. Ogoshi, *Chem. Soc. Rev.* **1997**, *26*, 355; c) M. W. Ward, *Chem. Soc. Rev.* **1997**, *26*, 365; d) P. Piotrowiak, *Chem. Soc. Rev.* **1999**, *28*, 143.

[8] a) S. Fukuzumi, *Pure Appl. Chem.* **2007**, *79*, 981; b) S. Fukuzumi, *Org. Biomol. Chem.* **2003**, *1*, 609; c) S. Fukuzumi, *Bull. Chem. Soc. Jpn.* **2006**, *79*, 177; d) S. Fukuzumi, T. Kojima, *J. Mater. Chem.* **2008**, *18*, 1427; e) S. Fukuzumi, *Phys. Chem. Chem. Phys.* **2008**, *10*, 2283; f) D. L. Feldheim, C. D. Keating, *Chem. Soc. Rev.* **1998**, *27*, 1; g) *Introduction of Molecular Electronics* (Eds.: M. C. Petty, M. R. Bryce), Oxford University Press, New York, **1995**; h) M. Emmelius, G. Pawlowski, H. W. Vollmann, *Angew. Chem.* **1989**, *101*, 1475; *Angew. Chem. Int. Ed. Engl.* **1989**, *28*, 1445. 18; i) S. Fukuzumi, T. Honda, K. Ohkubo, T. Kojima, *Dalton Trans.* **2009**, 3880.

[9] a) G. Kodis, P. A. Liddell, L. de La Garza, P. C. Clausen, J. S. Lindsey, A. L. Moore, T. A. Moore, D. Gust, *J. Phys. Chem. A* **2002**, *106*, 2036; b) D. Kuciauskas, P. A. Liddell, S. Lin, T. E. Johnson, S. J. Weghorn, J. S. Lindsey, A. L. Moore, T. A. Moore, D. Gust, *J. Am. Chem. Soc.* **1999**, *121*, 8604; c) P. A. Liddell, G. Kodis, L. de La Garza, A. L. Moore, T. A. Moore, D. Gust, *J. Phys. Chem. B* **2004**, *108*, 10256; d) G. Kodis, Y. Terazono, P. A. Liddell, J. Andreasson, V. Garg, M. Hambourger, A. L. Moore, T. A. Moore, D. Gust, *J. Am. Chem. Soc.* **2006**, *128*, 1818; e) M. Wolffs, F. J. M. Hoeben, E. H. A. Beckers, A. P. H. J. Schenning, E. W. Meijer, *J. Am. Chem. Soc.* **2005**, *127*, 13484.

[10] a) H. Imahori, Y. Sakata, *Adv. Mater.* **1997**, *9*, 537; b) M. Prato, *J. Mater. Chem.* **1997**, *7*, 1097; c) N. Martín, L. Sanchez, B. Illescas, I. Perez, *Chem. Rev.* **1998**, *98*, 2527; d) F. Diederich, M. Gomez-Lopez, *Chem. Soc. Rev.* **1999**, *28*, 263; e) H. Imahori, Y. Sakata, *Eur. J. Org. Chem.* **1999**, 2445; f) D. M. Guldi, *Chem. Commun.* **2000**, 321; g) D. M. Guldi, M. Prato, *Acc. Chem. Res.* **2000**, *33*, 695; h) D. M. Guldi, P. V. Kamat in *Fullerenes* (Eds.: K. M. Kadish, R. S. Ruoff), Wiley, New York, **2000**, Chapter 5, pp. 225–281; i) D. M. Guldi, *Chem. Soc. Rev.* **2002**, *31*, 22; j) M. D. Meijer, G. P. M. van Klink, G. van Koten, *Coord. Chem. Rev.* **2002**, *230*, 140; k) H. Imahori, S. Fukuzumi, *Adv. Funct. Mater.* **2004**, *14*, 525.

[11] a) M. R. Wasielewski, *Chem. Rev.* **1992**, *92*, 435; b) H. Kurreck, M. Huber, *Angew. Chem.* **1995**, *107*, 929; *Angew. Chem. Int. Ed. Engl.* **1995**, *34*, 849; c) P. D. W. Boyd, C. A Reed, *Acc. Chem. Res.* **2005**, *38*, 235; d) I. Bouamaied, T. Coskun, E. Stulz, *Struct. Bonding (Berlin)* **2006**, *121*, 1.

[12] a) S. Fukuzumi, K. Ohkubo, H. Imahori, J. Shao, Z. Ou, G. Zheng, Y. Chen, R. K. Pandey, M. Fujitsuka, O. Ito, K. M. Kadish, *J. Am. Chem. Soc.* **2001**, *123*, 10676; b) K. Ohkubo, H. Kotani, J. Shao, Z. Ou, K. M. Kadish, G. Li, R. K. Pandey, M. Fujitsuka, O. Ito, H. Imahori, S. Fukuzumi, *Angew. Chem.* **2004**, *116*, 871; *Angew. Chem. Int. Ed.* **2004**, *43*, 853; c) E. Maligaspe, N. V. Tkachenko, N. K. Subbaiyan, R. Chitta, M. E. Zandler, H. Lemmetyinen, F. D′Souza, *J. Phys. Chem. A* **2009**, *113*, 8478.

[13] a) M. E. El-Khouly, S. H. Shim, Y. Araki, O. Ito, K.-Y. Kay, *J. Phys. Chem. B* **2008**, *112*, 3910; b) J.-H. Kim, M. E. El-Khouly, Y. Araki, O. Ito, K.-Y. Kay, *Chem. Lett.* **2008**, *37*, 544; c) M. E. El-Khouly, J. B. Ryu, K.-Y. Kay, O. Ito, S. Fukuzumi, *J. Phys. Chem. C* **2009**, *113*, 15444.

[14] a) B. del Rey, T. Torres, *Tetrahedron Lett.* **1997**, *38*, 5351; b) C. G. Claessens, T. Torres, *J. Am. Chem. Soc.* **2002**, *124*, 14522; c) C. G. Claessens, D. González-Rodríguez, T. Torres, *Chem. Rev.* **2002**, *102*, 835; d) D. González-Rodríguez, T. Torres, D. M. Guldi, J. Rivera, L. Echegoyen, *Org. Lett.* **2002**, *4*, 335; e) D. González-Rodríguez, T. Torres, M. M. Olmstead, J. Rivera, M. A. Herranz, L. Echegoyen, C. Atienza Castellanos, D. M. Guldi, *J. Am. Chem. Soc.* **2006**, *128*, 10680; f) A. Medina, C. G. Glassens, G. M. Aminur Rahman, A. Lamsabhi, O. Mo, M. Yanez, D. M. Guldi, T. Torres, *Chem. Commun.* **2008**, 1759.

[15] a) M. E. El-Khouly, O. Ito, P. M. Smith, F. D′Souza, *J. Photochem. Photobiol. C* **2004**, *5*, 79; b) F. D′Souza, O. Ito, *Coord. Chem. Rev.* **2005**, *249*, 1410; c) R. Chitta, F. D′Souza, *J. Mater. Chem.* **2008**, *18*, 1440; d) F. D′Souza, O. Ito in *Handbook of Organic Electronics and Photonics, Vol. 1* (Ed.: H. S. Nalwa), American Scientific Publishers, Stevenson Ranch, **2008**, Chapter 13, pp. 485–521; e) Y. Araki, O. Ito in *Handbook of Organic Electronics and Photonics, Vol. 2* (Ed.: H. S. Nalwa), American Scientific Publishers: California, **2008**, Chapter 12, pp. 473–513; f) Y. Araki, O. Ito, *J. Photochem. Photobiol. C* **2008**, *9*, 93; g) F. D′Souza, O. Ito, *Chem. Commun.* **2009**, 4913; h) F. D′Souza, P. M. Smith, M. E. Zandler, A. L. McCarty, M. Itou, Y. Araki, O. Ito, *J. Am. Chem. Soc.* **2004**, *126*, 7898.

[16] *The Porphyrin Handbook* (Eds.: K. M. Kadish, K. M. Smith, R. Guilard), Academic Press, San Diego, **2000**, pp. 1–20.

[17] F. D′Souza, S. Gadde, D.-M. S. Islam, C. A. Wijesinghe, A. L. Schumacher, M. E. Zandler, Y. Araki, O. Ito, *J. Phys. Chem. A* **2007**, *111*, 8552.

[18] H. W. Kroto, J. R. Heath, S. C. O'Brien, R. F. Curl, R. E. Smalley, *Nature* **1985**, *318*, 162.

[19] a) H. Imahori, K. Hagiwara, T. Akiyama, M. Akoi, S. Taniguchi, T. Okada, M. Shirakawa, Y. Sakata, *Chem. Phys. Lett.* **1996**, *263*, 545; b) H. Imahori, M. E. El-Khouly, M. Fujitsuka, O. Ito, Y. Sakata, S. Fukuzumi, *J. Phys. Chem. A* **2001**, *105*, 325.

[20] a) F. D′Souza, G. R. Deviprasad, M. E. Zandler, V. T. Hoang, A. Klykov, M. VanStipdonk, A. Perera, M. E. El-Khouly, M. Fujitsuka, O. Ito, *J. Phys. Chem. A* **2002**, *106*, 3243; b) M. E. El-Khouly, L. M. Rogers, M. E. Zandler, G. Suresh, M. Fujitsuka, O. Ito, F. D′Souza, *ChemPhysChem* **2003**, *4*, 474.

[21] a) F. D′Souza, R. Chitta, K. Ohkubo, M. Tasior, N. K. Subbaiyan, M. E. Zandler, M. K. Rogachi, D. T. Gryko, S. Fukuzumi, *J. Am. Chem. Soc.* **2008**, *130*, 14263; b) F. D′Souza, E. Maligaspe, P. A. Karr, A. L. Schumacher, M. E. Ojaimi, C. P. Gros, J.-M. Barbe, K. Okubo, S. Fukuzumi, *Chem. Eur. J.* **2008**, *14*, 674.

[22] a) F. Ullmann, J. Bierlecki, *Ber. Dtsch. Chem. Ges.* **1901**, *34*, 2174; b) S. Gauthier, J. M. J. Frechet, *Synthesis* **1987**, 383.

[23] a) A. Vilsmeier, A. Haack, *Ber. Dtsch. Chem. Ges.* **1927**, *60*, 119; b) X.-C. Li, Y. Liu, M. S. Liu, A. K.-Y. Jen, *Chem. Mater.* **1999**, *11*, 1568.

[24] a) J. S. Lindsey, R. W. Wagner, *J. Org. Chem.* **1989**, *54*, 828; b) M. Gardner, A. J. Guerin, C. A. Hunter, U. Michelsen, C. Rotger, *New J. Chem.* **1999**, *23*, 309.

[25] The driving forces for charge recombination ($-\Delta G_{\mathrm{CR}}$) and charge separation ($-\Delta G_{\mathrm{CS}}$) were calculated according to the equations, $-\Delta G_{\mathrm{CR}} = E_{\mathrm{ox}} - E_{\mathrm{red}} - \Delta G_{\mathrm{S}}$ and $-\Delta G_{\mathrm{CS}} = E_{0,0} - (-\Delta G_{\mathrm{CR}})$; where E_{ox} is the first oxidation potential of the porphyrin, E_{red} is the first reduction potential of the fullerene and subphthalocyanine, $\Delta E_{0,0}$ is the energy of the 0–0 transition between the lowest excited state and the ground state of the porphyrin as evaluated from the fluorescence peaks. ΔG_{S} refers to the static energy, calculated by using the "dielectric continuum model" $\Delta G_{\mathrm{S}} = e^2/(4\pi\varepsilon_0\varepsilon_{\mathrm{S}}R_{\mathrm{Ct\text{-}Ct}})$. The symbols ε_0 and ε_{S} represent vacuum permittivity and dielectric constant of the solvent, respectively.

[26] a) F. D′Souza, S. Gadde, M. E. Zandler, K. Arkady, M. E. El-Khouly, M. Fujitusuka, O. Ito, *J. Phys. Chem. A* **2002**, *106*, 12393; b) F. D′Souza, M. E. El-Khouly, S. Gadde, A. L. McCarty, P. A. Karr, M. E. Zandler, Y. Araki, O. Ito, *J. Phys. Chem. B* **2005**, *109*, 10107.

[27] H. A. Benesi, J. H. Hildebrand, *J. Am. Chem. Soc.* **1949**, *71*, 2703.

[28] a) J. R. Miller, G. D. Dorough, *J. Am. Chem. Soc.* **1952**, *74*, 3977; b) K. M. Kadish, L. R. Shiue, *Inorg. Chem.* **1982**, *21*, 1112.

[29] a) R. A. Marcus, *J. Chem. Educ.* **1968**, *45*, 356; b) R. A. Marcus, N. Sutin, *Biochim. Biophys. Acta Rev. Bioenerg.* **1985**, *811*, 265; c) R. A. Marcus, *Angew. Chem.* **1993**, *105*, 1161; *Angew. Chem. Int. Ed. Engl.* **1993**, *32*, 1111; d) R. A. Marcus, *Rev. Mod. Phys.* **1993**, *65*, 599.

[30] S. Fukuzumi, K. Ohkubo, W. E, Z. Ou, J. Shao, K. M. Kadish, J. A. Hutchison, K. P. Ghiggino, P. J. Sintic, M. J. Crossley, *J. Am. Chem. Soc.* **2003**, *125*, 14984.

[31] a) I. R. Gould, J. E. Moser, B. Armitage, S. Farid, J. L. Goodman, M. S. Herman, *J. Am. Chem. Soc.* **1989**, *111*, 1917; b) C. C. Moser, J. M. Keske, K. Warncke, R. S. Farid, P. L. Dutton, *Nature* **1992**, *355*, 796; c) S. I. Khan, A. M. Oliver, M. N. Paddon-Row, Y. Rubin, *J. Am. Chem. Soc.* **1993**, *115*, 4919; d) R. M. Williams, J. M. Zwier, J. W. Verhoeven, *J. Am. Chem. Soc.* **1995**, *117*, 4093; e) R. D. Cannon, *Electron Transfer Reactions*, Butterworth, London, **1980**; f) W. Adam, A. Schönberger, *Chem. Ber.* **2006**, *139*, 2149.

Received: January 8, 2010
Published online: April 21, 2010